67-FM-16

NATIONAL AERONAUTICS AND SPACE ADMINISTRATION

MSC INTERNAL NOTE NO. 67-FM-16

February 3, 1967

ONE-WAY AND FLYBY INTERPLANETARY TRAJECTORY APPROXIMATIONS USING MATCHED CONIC TECHNIQUES

By Victor R. Bond and Ellis W. Henry

Advanced Mission Design Branch

MISSION PLANNING AND ANALYSIS DIVISION

MANNED SPACECRAFT CENTER
HOUSTON, TEXAS

MSC INTERNAL NOTE NO. 67-FM-16

ONE-WAY AND FLYBY INTERPLANETARY TRAJECTORY APPROXIMATIONS USING MATCHED CONIC TECHNIQUES

By Victor R. Bond and Ellis W. Henry
Advanced Mission Design Branch

February 3, 1967

MISSION PLANNING AND ANALYSIS DIVISION
NATIONAL AERONAUTICS AND SPACE ADMINISTRATION
MANNED SPACECRAFT CENTER
HOUSTON, TEXAS

Approved: Jack Funk
Jack Funk, Chief
Advanced Mission Design Branch

Approved: J. P. Mayer
John P. Mayer, Chief
Mission Planning and Analysis Division

CONTENTS

ONE-WAY AND FLYBY INTERPLANETARY TRAJECTORY APPROXIMATIONS USING MATCHED CONIC TECHNIQUES

By Victor R. Bond and Ellis W. Henry

SUMMARY

A method for matching the position and velocity components at the sphere of influence boundaries of both one-way and flyby trajectories is presented. A one-way matched conic is computed by specifying the Julian date of launch, flight time to the target planet, and the inclination and periapsis radii at both launch and target planet. A flyby matched conic trajectory is computed by specifying in addition the proper return time from the target planet to the launch planet and the return inclination and periapsis radius at the launch planet and by allowing the inclination and periapsis radius at the target planet to be free.

The matched conic trajectory that results is a good approximation to a precision trajectory and may be used as a reference for interplanetary guidance and navigation studies.

INTRODUCTION

This note will present the analysis which was done in Advanced Mission Design Branch (AMDB) in developing an interplanetary matched conic computer program. The output of the program is either the trajectory of a spacecraft between the Earth and another target planet, or a trajectory from Earth by way of a second planet and then back to Earth. These modes will be known as the one-way mode and the flyby mode, respectively.

The trajectory is separated into three distinct phases for each outbound or inbound leg. The first phase, called a planetocentric phase, begins at periapsis of the spacecraft trajectory about the launch planet and terminates at its sphere of influence. The second phase, called the heliocentric phase, begins at the launch planet sphere of influence and terminates at the target planet's sphere of influence. The third phase is also known as a planetocentric phase but the motion begins at the target planet's sphere of influence and terminates at periapsis near the target planet. The planetocentric phases assume the motion to be a conic with respect to either the launch or target planet, and the heliocentric phase assumes the motion to be a conic with respect to the Sun.

The purpose of the analysis presented will be to show how the positions and velocities are matched at the sphere of influence boundaries, and to outline the method of generating the conic trajectories during each phase of the trajectory. By matching both position and velocity, the resulting trajectory is a good approximation to a precise trajectory and as such may be used as a reference trajectory in navigation and guidance studies.

SYMBOLS

a	semi-major axis
e	eccentricity
F, G	functions occurring in solution of heliocentric two-body problem
f, g	functions occurring in solution of planetocentric two-body problem
H	hyperbolic equivalent of eccentric anomaly
$\hat{h}$	unit vector along angular momentum
i	inclination of orbital plane
$\hat{i}, \hat{j}, \hat{k}$	orthogonal unit vectors defining an inertial system

$\hat{n}$	unit vector along nodal line
$\underline{R}$, $\underline{V}$	heliocentric position and velocity vectors
$\underline{r}$, $\underline{v}$	planetocentric position and velocity vectors
r	magnitude of $\underline{r}$
$\hat{S}$	unit vector outward from planet along hyperbolic asymptote
T	Julian date
t	time
$\hat{W}$	unit vector shown in figure 1
α, δ	right ascension and declination of hyperbolic asymptote
$\underline{\zeta}$	vector along angular momentum defined by equation (19)
η	angle between periapsis and the hyperbolic asymptote
μ	constant of gravitation
ν	angle between semilatus rectum and velocity vector
σ	angle defined by equation (17)

Subcripts

A	quantity referenced to arrival planet
D	quantity referenced to departure on launch planet
F	quantity computed at target planet in free-return mode
FL	flight
P	denoting planet position or velocity referenced to Sun
R	quantity specified at Earth for return leg of free-return mode
T	quantity referred to target planet in free-return mode
π	quantity computed or specified at periapsis

x, y, z	components of a vector in system defined by $\hat{i}$, $\hat{j}$, $\hat{k}$
1, 2	quantity in neighborhood of planetary sphere of influence

Superscripts

$( )^*$	quantity at planetary sphere of influence
$( )^{*'}$	quantity at planetary sphere of influence, evaluated from heliocentric conic
$( )^+$	quantity referring to northern hemisphere of planet
$( )^-$	quantity referring to southern hemisphere of planet

ANALYSIS

This analysis, with some changes, is similar to that presented in reference 1. The authors of reference 1 restricted themselves to the one-way class of trajectories. As mentioned above, the flyby mode is presented here. Another slight difference is that the inclination in the planetocentric phase is specified rather than the right ascension of ascending mode, which was specified in reference 1. The mathematical approach to the problem is also different. The authors of reference 1 solved the problem without resorting to the convenience of vector notation, which is used to the fullest extent in this note.

For the one-way mode, the following quantities are specified: the Julian date of launch from the departure plane, T_D; the flight time to the target planet, t_{FLA}; the inclination, i_D, and radius of periapsis, $r_{\pi D}$, at the departure planet; and the inclination, i_A, and radius of periapsis, $r_{\pi A}$, at the arrival, or target planet. These six quantities are sufficient information to completely solve for the trajectory in the one-way mode except for bounds on the inclinations, which will be discussed later.

For the flyby mode, the following quantities are specified: the Julian date for launch from Earth, T_D; the flight time to the target planet, t_{FLA}; the flight time to return to Earth from the target planet, t_{FLR}; the inclination, i_D, and radius of periapsis, $r_{\pi D}$, at

Earth departure; the inclination, i_R, and radius of periapsis, $r_{\pi R}$, at Earth return. There are seven quantities specified here but they are subject to the single constraint that the flight times must be chosen such that the incoming velocity magnitude at the target planet's sphere of influence must be equal to the outgoing velocity magnitude at the sphere of influence. The values of T_D, t_{FLA}, and t_{FLR} may be picked from several documented sources such as references 2 and 3.

The analyses for the separate trajectory phases are done in the following two sections.

The Planetocentric Phases

During this phase, the spacecraft motion is assumed to be planet-centered. The necessary quantities for determining the trajectory in the planetocentric phase are the velocity of the spacecraft at the planetary sphere of influence as computed from a heliocentric trajectory $\underline{v}^{*\prime}$, the radius of the sphere of influence, r^*, the radius of periapsis, r_π, and the inclination of the trajectory plane to the planetary equator, i.

If the launch date, arrival date at target planet, and return date to Earth are chosen so that the trajectory is a flyby, the inclination, i, and periapsis radius, r_π, at the target planet are not independent quantities and may be computed as will be shown later.

The solution of this problem must ultimately yield the position and velocity vectors $\underline{r}^*$ and $\underline{v}^*$ of the spacecraft at the sphere of influence. It should be noted that the velocity $\underline{v}^*$ is slightly different in direction and magnitude from the velocity $\underline{v}^{*\prime}$. This difference is due to the fact that $\underline{v}^{*\prime}$ was computed from a heliocentric trajectory which goes through the center of a massless planet, while $\underline{v}^*$ assumes two-body motion about the planet with a non-zero periapsis radius.

The semi-major axis is computed from,

$$a^{-1} = \left(\frac{2}{r^*} - \frac{v^{*\prime 2}}{\mu} \right), \tag{1}$$

which will, of course, be negative since all of the trajectories in the planetocentric phase will be hyperbolic.

The eccentricity is found from

$$e = 1 - \frac{r_\pi}{a} . \tag{2}$$

As shown in figure (1), the angle between $\underline{r}_\pi$ and the asymptote of the hyperbola is

$$\eta = \cos^{-1}\left(\frac{-1}{e}\right). \tag{3}$$

The time from periapsis to the sphere of influence is

$$t_\pi = \sqrt{\frac{-a^3}{\mu}}\,(e \sin H - H), \tag{4}$$

where H is found from

$$\cosh H = \left(1 - \frac{r^*}{a}\right)\frac{1}{e} . \tag{5}$$

The magnitude of the velocity at periapsis is found from

$$v_\pi = \sqrt{\mu\left(\frac{2}{r_\pi} - \frac{1}{a}\right)} . \tag{6}$$

The directions of the hyperbolic asymptotes which are always assumed to have their origin at the planet may be computed by making the assumption that $\underline{v}^{*\prime}$ is parallel to the hyperbolic asymptote for departure trajectories and anti-parallel for arrival trajectories. In vector notation,

$$\hat{S}_D = \frac{\underline{v}^{*\prime}_D}{v^{*\prime}} \tag{7}$$

for departure, and

$$\hat{S}_A = \frac{-\underline{v}^{*\prime}_A}{v^{*\prime}} \tag{8}$$

for arrival.

In order to compute the planetocentric position and velocity vectors $\underline{r}_D^*$ and $\underline{v}_D^*$ or $\underline{r}_A^*$ and $\underline{v}_A^*$, it is first necessary to derive expressions for the position and velocity at periapsis. For the departure case, see figure 1(a) and for the arrival case see figure 1(b).

The derivation of $\underline{r}_\pi$ and $\underline{v}_\pi$ is essentially trigonometrical and the results are stated simply as

$$\left.\begin{aligned} \underline{r}_{\pi D} &= r_{\pi D}\left(\cos\eta\,\hat{S}_D - \sin\eta\,\hat{W}_D\right) \\ \underline{v}_{\pi D} &= v_{\pi D}\left(\sin\eta\,\hat{S}_D + \cos\eta\,\hat{W}_D\right) \end{aligned}\right\} \tag{9}$$

for departure trajectories, and

$$\left.\begin{aligned} \underline{r}_{\pi A} &= r_{\pi A}\left(\cos\eta\,\hat{S}_A - \sin\eta\,\hat{W}_A\right) \\ \underline{v}_{\pi A} &= v_{\pi A}\left(-\sin\eta\,\hat{S}_A - \cos\eta\,\hat{W}_A\right) \end{aligned}\right\} \tag{10}$$

for arrival trajectories.

The unit vectors $\hat{W}_D$ and $\hat{W}_A$ for the arrival and departure are found from

$$\left.\begin{aligned} \hat{W}_D &= \hat{h} \times \hat{S}_D \\ \hat{W}_A &= -\hat{h} \times \hat{S}_A \end{aligned}\right\} \tag{11}$$

$\hat{W}_D$ or $\hat{W}_A$ is in the plane of the motion perpendicular to $\underline{v}^{*\prime}$, and the vector $\hat{h}$ is a unit vector normal to the plane of motion and has the same direction as the angular momentum. The unit vector $\hat{h}$ depends upon the orientation of the plane of motion with respect to the planetocentric inertial coordinate system and is given by (ref. 4)

$$\hat{h} = \hat{i}\sin\Omega\sin i - \hat{j}\cos\Omega\sin i + \hat{k}\cos i \tag{12}$$

The unit vector $\hat{i}$ is along an inertial direction is space, for example, the vernal equinox if the system is geocentric; $\hat{k}$ is normal to the

planet's equator and in the same direction as the planetary spin axis; and $\hat{j}$ is chosen to complete the right-hand system.

Now specialize to the one-way mission case; that is, the trajectory is not a flyby or free return. The inclination, i, is specified as either i_D or i_A and the right ascension of the ascending mode, Ω, may be computed except for an ambiguity which may be resolved by arbitrary selection.

For departure trajectories, as may be seen from figure 2(a), the periapsis may be chosen to be in either the northern hemisphere or the southern hemisphere by specifying either

$$\Omega^{+} = \alpha + \sigma + \pi \tag{13}$$

for northern hemisphere periapsis, or

$$\Omega^{-} = \alpha - \sigma \tag{14}$$

for southern hemisphere periapsis.

For arrival trajectories, as seen from figure 2(b)

$$\Omega^{+} = \alpha - \sigma \tag{15}$$

for nothern hemisphere periapsis, and

$$\Omega^{-} = \alpha + \sigma + \pi \tag{16}$$

for southern hemisphere periapsis.

The angle σ is found in all cases from,

$$\sin \sigma = \frac{\tan \delta}{\tan i} \tag{17}$$

The angles δ and α are the declination and right ascension of the asymptote and may be computed from $\hat{S}_D$ or $\hat{S}_A$.

Equation (16) expresses the limitation on the angle of inclination, which may be specified. It is obvious that

$$|\tan \delta| < |\tan i| \tag{18}$$

for (16) to be meaningful.

For the flyby case, the inclination, the periapsis radius, and the right ascension of the ascending node are computed from the arrival and departure velocity vectors at the target planet, $\underline{v}^{*'}_{AT}$ and $\underline{v}^{*'}_{DT}$, which of course must have the same magnitudes. The cross product $\underline{\zeta} = \underline{v}^{*'}_{AT} \times \underline{v}^{*'}_{DT}$ must have the same direction as the angular momentum,

$$\hat{h} = \frac{\underline{v}^{*'}_{AT} \times \underline{v}^{*'}_{DT}}{\left|\underline{v}^{*'}_{AT} \times \underline{v}^{*'}_{DT}\right|} = \frac{\underline{\zeta}}{\zeta} . \tag{19}$$

The inclination is computed by comparing equations (12) and (19),

$$\hat{k} \cdot \hat{h} = \cos i_F = \zeta_z / \zeta . \tag{20}$$

Similarly, the right ascension of the ascending node is found from the two equations,

$$\left.\begin{aligned} \sin \Omega \ \sin i_F &= \frac{\zeta_x}{\zeta} \\ \cos \Omega \ \sin i_F &= -\frac{\zeta_y}{\zeta} \end{aligned}\right\} \tag{21}$$

The radius of periapsis, $r_{\pi F}$, is found by first finding the semi-major axis from (1), and the eccentricity by inverting (3), i. e.,

$$e = \frac{-1}{\cos \eta} . \tag{22}$$

From figure 3, it is seen that ζ is related to the angle ν by

$$\eta = \nu + \frac{\pi}{2} , \tag{23}$$

where ν is found from the magnitude of the cross-product in equation (19),

$$\sin 2\nu = \frac{\left|\underline{v}^{*'}_{AT} \times \underline{v}^{*'}_{DT}\right|}{v^{*'2}} . \tag{24}$$

From equations (2), (22), and (24),

$$r_{\pi F} = a\left(1 - \csc \nu\right) . \tag{25}$$

The computed inclination i_F and periapsis radius $r_{\pi F}$ at the flyby planet are now used exactly as in the one-way case. For the Earth-target planet leg i_D and $r_{\pi D}$ are specified, the target arrival inclination and periapsis radius are set as $i_A = i_F$ and $r_{\pi A} = r_{\pi F}$. For the target planet-Earth leg, $i_D = i_F$ and $r_{\pi D} = r_{\pi F}$ and $i_A = i_R$ and $r_{\pi A} = r_{\pi R}$, where i_R and $r_{\pi R}$ are, of course, specified.

The one-way case and the flyby case reduce to the same formulation with the exception noted above. The perigee position and velocity vectors equations (9) or (10) are now advanced (for departure trajectories) or regressed (for arrival cases) to the sphere of influence of the planet.

For departure trajectories,

$$\left.\begin{aligned} \underline{r}_D^* &= \underline{r}_{\pi D} f\left(t_{\pi D}\right) + \underline{v}_{\pi D} g\left(t_{\pi D}\right) \\ \underline{v}_D^* &= \underline{r}_{\pi D} \dot{f}\left(t_{\pi D}\right) + \underline{v}_{\pi D} \dot{g}\left(t_{\pi D}\right) \end{aligned}\right\} \tag{26}$$

and, for arrival trajectories,

$$\left.\begin{aligned} \underline{r}_A^* &= \underline{r}_{\pi A} f\left(-t_{\pi A}\right) + \underline{v}_{\pi A} g\left(-t_{\pi A}\right) \\ \underline{v}_A^* &= \underline{r}_{\pi D} \dot{f}\left(-t_{\pi A}\right) + \underline{v}_{\pi A} \dot{g}\left(-t_{\pi A}\right) \end{aligned}\right\} \tag{27}$$

The Heliocentric Phase

During this phase, the spacecraft motion is assumed to be Sun-centered and to take place between the sphere of influence of the departure and arrival planets. Basically, this solution involves the solution of Lambert's problem.

The quantities that are required from this phase for use in the planetocentric phases are the velocities $\underline{v}_D^{*\prime}$ and $\underline{v}_A^{*\prime}$ of the spacecraft at the planetary spheres of influence. These velocities are estimated

initially as given in the Appendix. After their first computation, the matching process begins, and they are subsequently computed as follows:

Let $\underline{r}^*_D$ and $\underline{r}^*_A$ be the position vectors of the spacecraft at the departure and arrival planetary spheres of influence (taken to be with respect to their respective planets, of course). Further, let $t_{\pi D}$ and $t_{\pi A}$ be the time to periapsis from the spheres of influence of the departure and arrival planets. These quantities, $\underline{r}^*_D$, $\underline{r}^*_A$, $t_{\pi D}$, and $t_{\pi A}$ are computed with respect to the planets as shown in the section on the planetocentric phase.

The heliocentric portion of the flight must now be computed with slightly difference position vectors for the spacecraft as well as at slightly different times at the spheres of influence.

The adjusted position vectors of the spacecraft with respect to the Sun at the planetary spheres of influence are

$$\underline{R}^{*\prime}_D = \underline{R}_D\left(T^{*\prime}_D\right) = \underline{r}^*_D + \underline{R}_{PD}\left(T^{*\prime}_D\right) \tag{28}$$

and

$$\underline{R}^{*\prime}_A = \underline{R}_A\left(T^{*\prime}_A\right) = r^*_A + \underline{R}_{PA}\left(T^{*\prime}_A\right), \tag{29}$$

where

$$T^{*\prime}_D = T_D + t_{\pi D}$$

$$T^{*\prime}_A = T_A + t_{\pi A}\,.$$

The position vectors $\underline{R}^{*\prime}_D$ and $\underline{R}^{*\prime}_A$ and the time $T^{*\prime}_A - T^{*\prime}_D$ are now used to solve Lambert's problem. The result of this solution is the spacecraft arrival and departure velocities at the sphere of influence, that is, $\underline{V}^{*\prime}_D$ and $\underline{V}^{*\prime}_A$. The velocity vectors of the spacecraft with respect to the planets may be found by

$$\underline{v}^{*\prime}_D = \underline{V}^{*\prime}_D - \underline{V}_{PD}\left(T^{*\prime}_D\right) \tag{30}$$

and

$$\underline{v}^{*\prime}_A = \underline{V}^{*\prime}_A - \underline{V}_{PA}\left(T^{*\prime}_A\right). \tag{31}$$

THE VELOCITY MATCH PROCESS

The relative velocity vectors $\underset{\rightarrow}{v}^{*'}_D$ and $\underset{\rightarrow}{v}^{*'}_A$ at the sphere of influence of the departure and arrival planets which were computed in the heliocentric phase assuming massless planets must now be compared with the velocity vectors $\underset{\rightarrow}{v}^{*}_D$ and $\underset{\rightarrow}{v}^{*}_A$, which were computed during the planetocentric phases. If $\left|\underset{\rightarrow}{v}^{*}_D - \underset{\rightarrow}{v}^{*'}_D\right|$ and $\left|\underset{\rightarrow}{v}^{*}_A - \underset{\rightarrow}{v}^{*'}_A\right|$ are less than a small velocity tolerance (say, 3 fps), then the velocities are considered to be matched and the entire problem is solved. If either or both of the velocity differences are greater than the tolerance, then the planetocentric phases are repeated and the computations are initiated by $\underset{\rightarrow}{v}^{*'}_D$ and $\underset{\rightarrow}{v}^{*'}_A$. It has been found that a velocity match is attained to within 3 fps after only two or three cycles. The matching process can be visualized easily from figure 4.

For the flyby case, the Earth departure and Earth return legs are treated separately, being certain that the periapsis radius, inclination, and right ascension of ascending node are the same for both legs. It has generally been found that it is not necessary to repeat the calculation of these quantities for each matching cycle. These are computed from $\underset{\rightarrow}{v}^{*'}_D$ and $\underset{\rightarrow}{v}^{*'}_A$ just prior to the first cycle and are then maintained throughout.

AN EXAMPLE

The short-long Mars flyby mission (i.e., short outgoing trajectory and long return trajectory) with a launch date of September 20, 1975, was chosen as an example. From reference 2, it is seen that this mission has a near minimum injection velocity at Earth. This mission is designated by the following specified quantities:

T_D = 2 442 675.0 (September 20, 1975)

t_{FLA} = 133.29 days

t_{FLR} = 538.64 days

$i_D = 60^\circ$

$r_{\pi D}$ = 262 n. mi. plus radius of Earth

$i_R = 60^\circ$

$r_{\pi R}$ = 70 n. mi. plus radius of Earth

Two trajectories were computed using the above input. The first required the periapsis at Earth injection to be in the southern hemisphere and the periapsis at Earth return to be in the southern hemisphere. The second required a north periapsis injection at Earth and a south periapsis return at Earth. The coordinate system used in all phases was the equatorial system. These trajectories are summarized in table I.

CONCLUDING REMARKS

A method for matching conic trajectories at sphere of influence boundaries has been presented. The match is exact for position components and within about 3 fps (root sum square) for the velocity components. By specifying the Julian date of launch, flight time to the target planet, and the inclinations and periapsis radii at both launch and target planet, a one-way match conic trajectory may be computed. By further specifying the proper return time from the target planet to Earth, the return inclination and periapsis radius at Earth, and allowing the inclination and periapsis radius at the target planet to be free, a flyby matched conic trajectory may be computed.

When the inclination and periapsis radius are specified at a planet, there are two possible trajectories in that planet's sphere of influence. This ambiguity arises due to fact that for a given inclination there exists two possible values of the right ascension of the ascending node. By proper choice of this angle, the periapsis position vector may be placed in either the northern or southern hemisphere.

The resulting trajectory is a good approximation to a precision trajectory and may be used as a reference trajectory for interplanetary guidance and navigation studies.

APPENDIX

THE FIRST ESTIMATES OF THE SPACECRAFT DEPARTURE AND ARRIVAL RELATIVE VELOCITIES

The first step in estimating $\underline{v}_D^{*\prime}$ and $\underline{v}_A^{*\prime}$ is to obtain the conic solution for the motion of the spacecraft between the centers of departure and arrival planets. Given the Julian date, T_D, of launch from the departure plane, and the Julian date, T_A, at the arrival planet, the initial and final position vector, $\underline{R}_D$ and $\underline{R}_A$, of the spacecraft are determined from the planetary ephemeris. By the solution of Lambert's problem, the corresponding velocities $\underline{V}_D$ and $\underline{V}_A$ are found. (This solution is given for example in ref. 7.) The velocities $\underline{V}_D^*$ or $\underline{V}_A^*$ may be determined from $\underline{R}_D$ and $\underline{V}_D$, or $\underline{R}_A$ and $\underline{V}_A$ by numerically determining the time, t*, required by the spacecraft to travel from the center of the departure planet to its sphere of influence, or from the arrival planet's sphere of influence to its center.

The position and velocity, $\underline{R}_D$ and $\underline{V}_D$ at departure or $\underline{R}_A$ and $\underline{V}_A$ at arrival, are used as initial conditions to determine the spacecraft's heliocentric position $\underline{R}_1$, at some time t_1, near the sphere of influence.

For departure,

$$\underline{R}_1 (t_1) = \underline{R}_D F(t_1) + \underline{V}_D G(t_1). \tag{A1}$$

The relative position of the spacecraft with respect to the planet at t_1 is computed from

$$\underline{r}_1(t_1) = \underline{R}_1(t_1) - \underline{R}_{PD} (t_1 + T_D). \tag{A2}$$

Now let t be incremented a small amount Δt, and again compute the relative position at $t_2 = t_1 + \Delta t$;

$$\underline{r}_2(t_2) = \underline{R}_2(t_2) - \underline{R}_{PD}(t_2 + T_D). \tag{A3}$$

The planetary ephemeris may be obtained analytically as in reference 5 or numerically from a planetary data source as in reference 6.

The rate of change of the relative spacecraft position magnitude is fairly linear near the sphere of influence so that the time of crossing the sphere of influence is given approximately by

$$t^* = t_1 + \frac{t_2 - t_1}{r_2 - r_1} (r^* - r_1) . \tag{A4}$$

Experience has shown that t_1 may be taken to be 1 day and Δt as 1 hour to give a fairly accurate value of t^*. This may be improved by repeating the computation in (A4) by letting $t_1 = t^*$ and letting Δt be 1 minute. After 2 cycles of this computation t^* is such that the computed value of r^* is within 20 n. mi. of the actual value.

The relative position $\underline{r}_D^{*\prime}$ and velocity $\underline{v}_D^{*\prime}$ at the departure sphere of influence may now be computed from

$$\begin{aligned} \underline{r}_D^{*\prime}(t^*) &= \underline{R}^*(t^*) - \underline{R}_{PD} (t^* + T_D) \\ \text{and} \qquad \underline{v}_D^{*\prime}(t^*) &= \underline{V}^*(t^*) - \underline{V}_{PD} (t^* + T_D), \end{aligned} \tag{A5}$$

where

$$\begin{aligned} \underline{R}^* (t^*) &= \underline{R}_D F(t^*) + \underline{V}_D G(t^*), \\ \underline{V}^* (t^*) &= \dot{\underline{R}}_D F(t^*) + \dot{\underline{V}}_D G(t^*), \end{aligned}$$

and $\underline{R}_{PD}(t^* + T_D)$ and $\underline{V}_{PD}(t^* + T_D)$ are determined from the planetary ephemeris.

The relative position and velocity, $\underline{r}_A^{*\prime}$ and $\underline{v}_A^{*\prime}$, at the arrival sphere of influence are computed similarly, with t_1 and Δt taken to be negative and with $\underline{R}_A$ and $\underline{V}_A$ as the initial conditions.

TABLE I.- MARS FLYBY TRAJECTORY FOR A

SEPTEMBER 20, 1975 LAUNCH DATE

Julian Date	Point of interest	Position components[a]			Position magnitude, n. mi.	Velocity components, fps			Velocity magnitude, fps
		x	y	z		$\dot{x}$	$\dot{y}$	$\dot{z}$	
(a) South periapsis launch; south periapsis return									
2442675.0000	Periapsis at Earth (Planetccentric)	1703.6211	-728.81447	-3209.4309	3705.9333	15849.482	36896.013	34.637368	40156.233
2442676.7653	ESCI (Planetccentric)	11955.585	421955.73	269774.76	500967.05	280.08468	16108.928	10579.718	19274.502
2442676.7653	ESCI (Heliocentric)	1.0033357	-.032447015	-.012994972	1.0039443	2681.1013	105374.68	49288.564	116363.11
2442807.5037	MSCI (Heliocentric)	-.41486301	1.4017195	.65466946	1.6017244	-79116.803	12260.434	5562.1728	80254.123
2442807.5037	MSOI (Planetocentric)	59531.582	-287962.87	-106974.11	312905.87	-5405.1442	25579.753	9685.8969	27881.103
2442808.2900	Periapsis at Mars (Planetocentric)	-1022.7876	-512.97625	1579.4828	1950.3859	-3879.7633	30981.483	7549.6806	32123.239
2442809.0771	MSOI (Planetocentric)	-15348.746	310039.79	38857.806	312842.10	-1258.9020	27621.415	3291.6776	27845.331
2442809.0771	MSOI (Heliocentric)	-.43616847	1.4053093	.65527458	1.6107520	-74698.962	13406.474	-1250.1661	75902.775
2443345.8253	ESOI (Heliocentric)	.48428242	-.82395646	-.35989325	1.0212526	82592.902	64166.510	40821.195	112273.32
2443345.8253	ESOI (Planetocentric)	31543.075	-344494.56	-360582.25	499690.94	-1750.9221	21788.573	22446.611	31331.421
2443346.9300	Periapsis at Earth (Planetocentric)	2088.2634	2772.7022	-546.81446	3513.9333	-15487.868	19706.441	40776.797	47864.027

[a]Planetocentric points of interest are measured in n. mi.
Heliocentric points of interest are measured in A.U.

TABLE I.- MARS FLYBY TRAJECTORY FOR A

SEPTEMBER 20, 1975 LAUNCH DATE

Julian Date	Point of interest	Position components[a]			Position magnitude, n. mi.	Velocity components, fps			Velocity magnitude, fps
		x	y	z		$\dot{x}$	$\dot{y}$	$\dot{z}$	
(b) North periapsis launch; south periapsis return									
2442675.0000	Periapse at Earth (Planetocentric)	1660.0373	-3252.4149	632.46753	3705.9332	15465.263	14523.605	34094.835	40156.782
2442676.7652	ESOI (Planetocentric)	11866.103	415046.54	280291.31	500966.71	281.17171	16105.432	10587.093	19275.646
2442676.7652	ESOI (Heliocentric)	1.0033346	-.032532549	-.012864779	1.0039443	2682.2971	105372.69	49293.568	116363.45
2442807.5037	MSOI (Heliocentric)	-.41486301	1.4017190	.65467098	1.6017246	-79117.159	12265.999	5551.8577	80254.611
2442807.5037	MSOI (Planetocentric)	59531.271	-288002.76	-106851.27	312900.54	-5405.5459	25585.348	9675.7206	27382.782
2442808.2900	Periapse at Mars (Planetocentric)	-1022.9169	-512.33883	1579.6059	1950.3858	-3879.9646	30985.913	7537.5797	32124.695
2442809.0771	MSOI (Planetocentric)	-15348.746	310039.79	38857.806	312842.10	-1258.9020	27621.415	3291.6776	27845.331
2442809.0771	MSOI (Heliocentric)	-.43616847	1.4053093	.65527458	1.6107520	-74698.962	13406.474	-1250.1661	75902.775
2443345.8253	ESOI (Heliocentric)	.48428242	-.82395646	-.35989325	1.0212526	82592.902	64166.510	40821.195	112273.32
2443345.8253	ESOI (Planetocentric)	31543.075	-344494.56	-360582.25	499690.94	-1750.9221	21788.573	22446.611	31331.421
2443346.9300	Periapse at Earth (Planetocentric)	2088.2634	2772.7022	-546.81446	3513.9333	-15487.868	19706.441	40776.797	47864.027

[a]Planetocentric points of interest are measured in n. mi.
Heliocentric points of interest are measured in A.U.

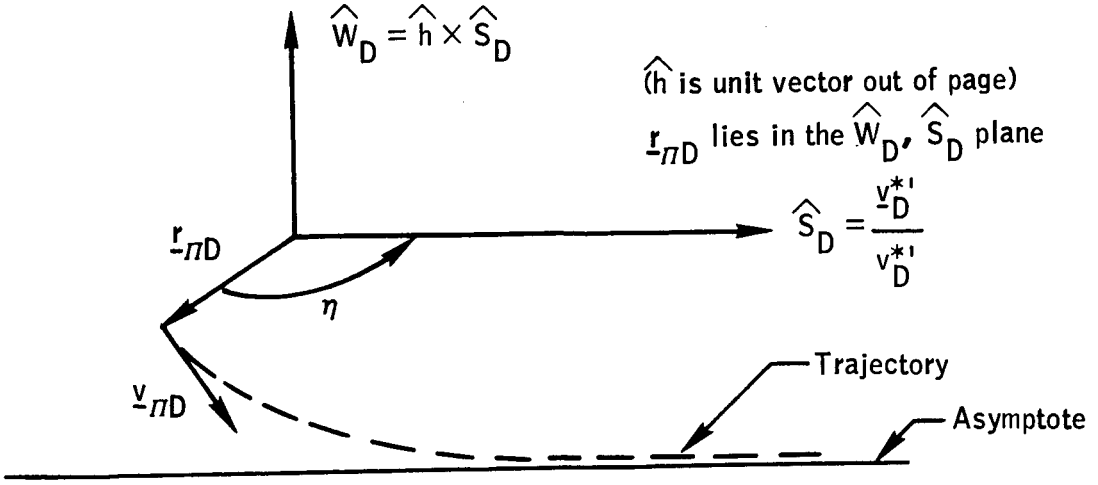

(a) Departing

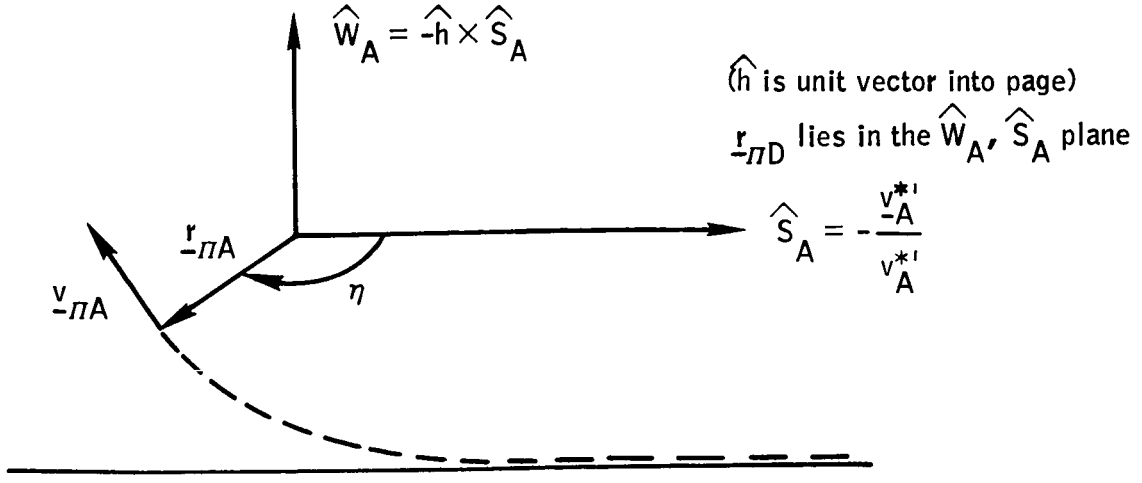

(b) Arriving

Figure 1. - Geometry of hyperbolic trajectory.

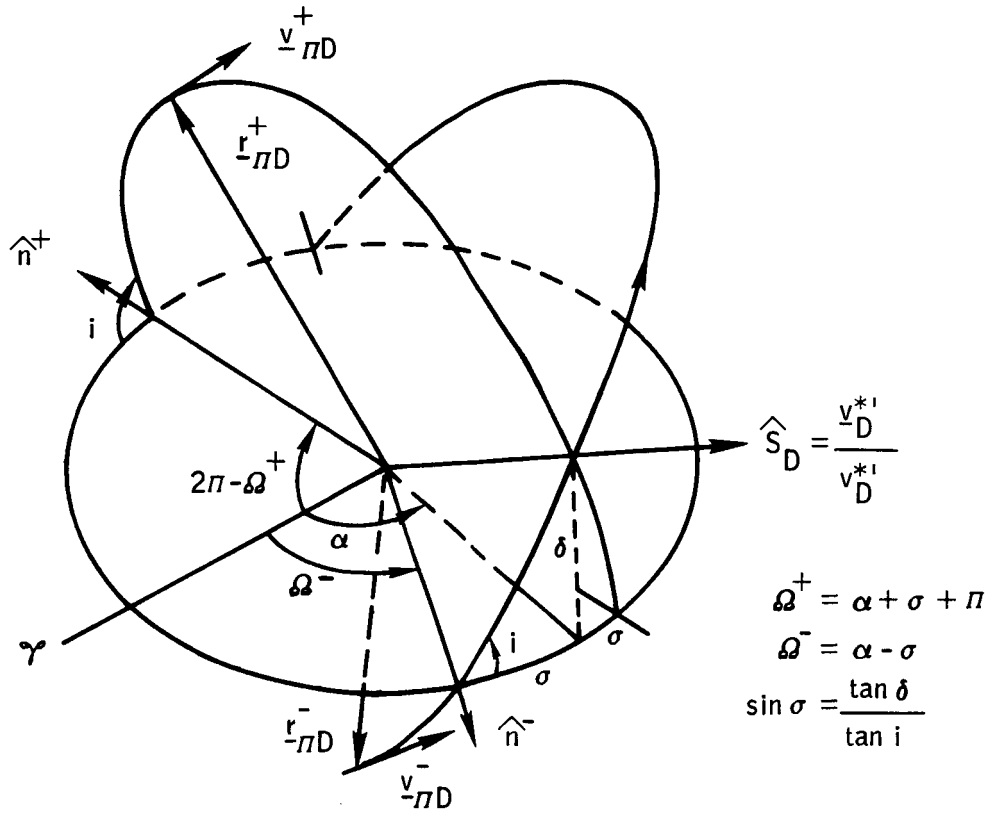

(a) Departing

Figure 2. - Geometry of northern (+) and southern (-) periapsis vectors for hyperbolic trajectories.

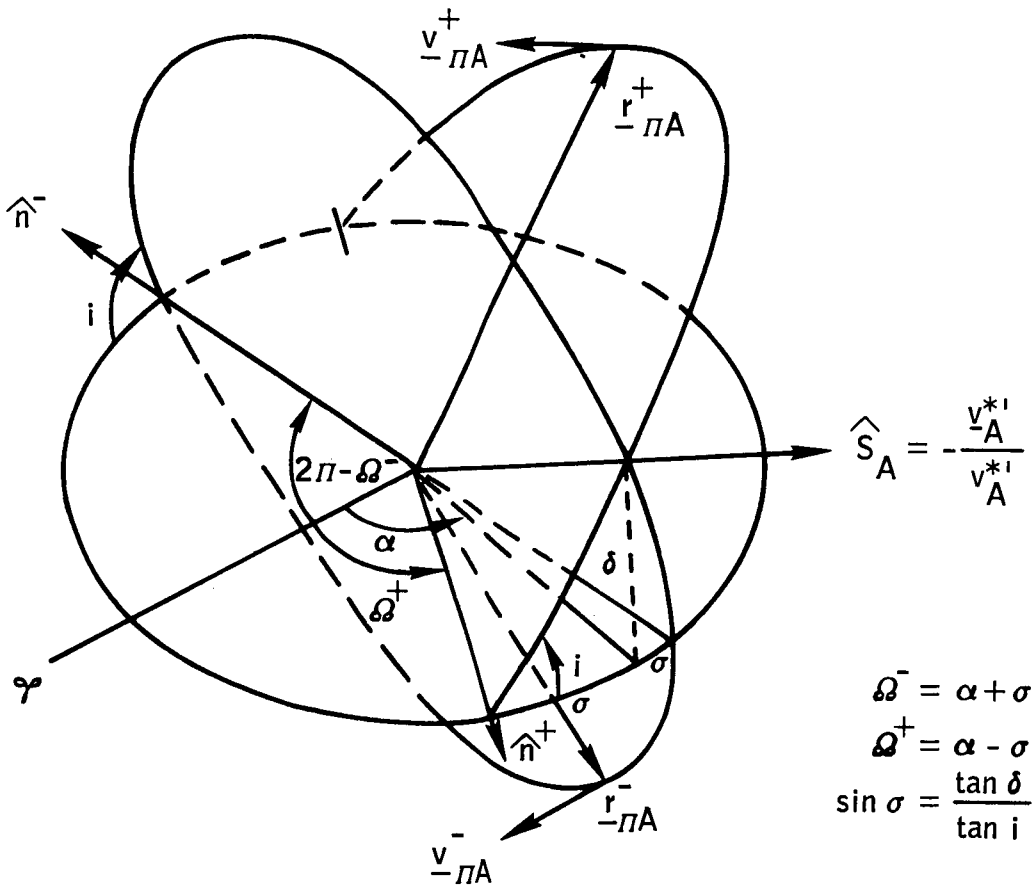

(b) Arriving

Figure 2. - Concluded.

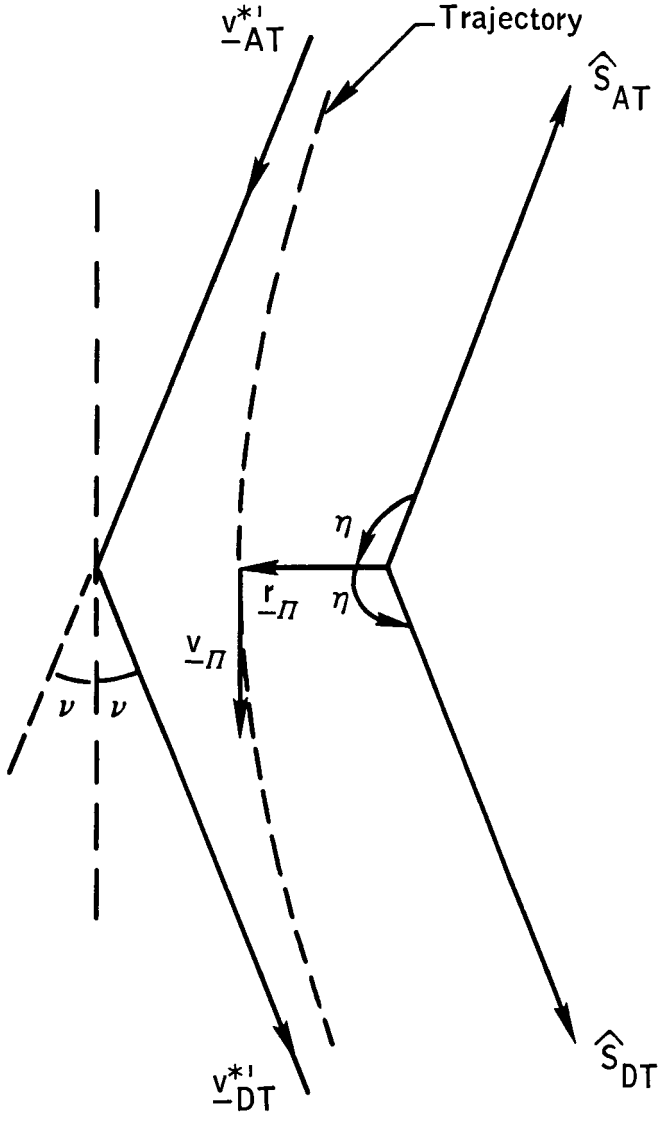

Constraint: $\left|\underline{v}^{*\prime}_{AT}\right| = \left|\underline{v}^{*\prime}_{DT}\right|$

Figure 3. - Geometry of flyby hyperbolic trajectory.

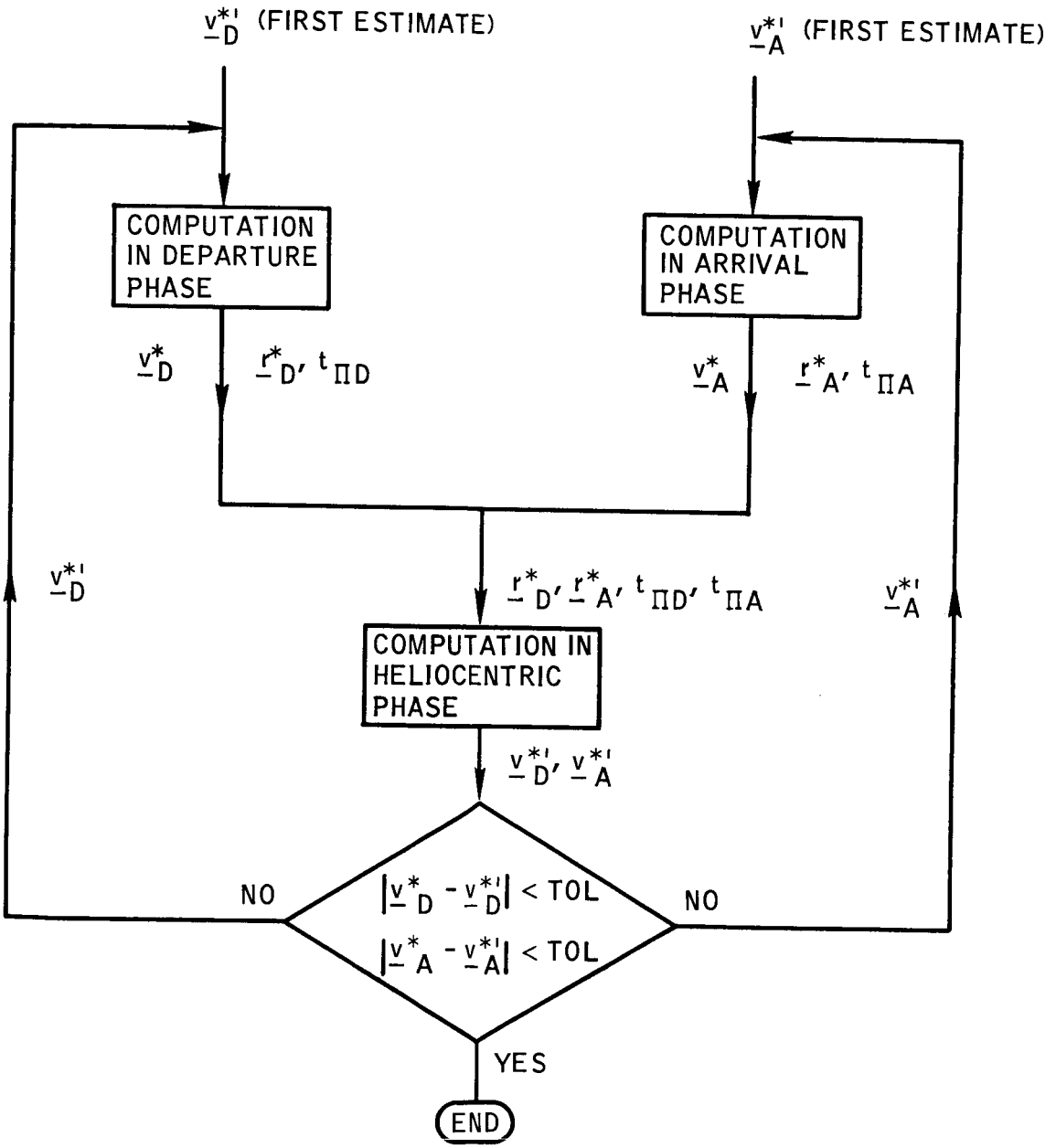

Figure 4. - Velocity mathing of heliocentric phase with planetocentric phases.

REFERENCES

1. Knip, G. Jr.; and Zola, C. L.: Three-Dimensional Sphere-of-Influence Analysis of Interplanetary Trajectories to Mars, NASA TN D-1199, May 1962.

2. Garland, B. J.: Free Return Trajectories to Mars Between 1975 and 1982, MSC IN No. 66-FM-141, November 25, 1966.

3. Lockheed Missiles and Space Company: Planetary Flight Handbook, NASA SP-35, parts 1, 2, 3. August 1963.

4. Danby, John M. A.: Fundamentals of Celestial Mechanics. The Macmillan Company, 1962.

5. Garland, B. J.: Three-Dimensional Trajectory Analysis of Nonstop Round-Trip Mars Mission Between 1970 and 1988 using Propulsive-Gravity Turns with Atmospheric Effects, NASA TM X-1122, August 1965.

6. Henry, E. W.: A Double Precision Fortran Computer Program (GPFEM) for a General Purpose Lunar and Planetary Ephemeris, MSC-IN No. 67-FM-8, January 19, 1967.

7. Battin, R. H.: Astronautical Guidance. McGraw-Hill Book Company, Inc. 1964.